

# Wavelet analogue of the Ginzburg-Landau energy and its $\Gamma$ -convergence

J. A. Dobrosotskaya, A. L. Bertozzi

## Abstract

This paper considers a wavelet analogue of the classical Ginzburg-Landau energy, where the  $H^1$ -seminorm is replaced by the Besov seminorm defined via an arbitrary regular wavelet. We prove that functionals of this type converge, in the  $\Gamma$ -sense, to a weighted analogue of the TV functional on characteristic functions of finite-perimeter sets. The  $\Gamma$ -limiting functional is defined explicitly, in terms of the wavelet that is used to define the energy. We show that the limiting energy is none other than the surface tension energy in the 2D Wulff problem and its minimizers are represented by corresponding Wulff shapes. This fact as well as the  $\Gamma$ -convergence results are illustrated with a series of computational examples.

## 1 Introduction

Fourier analysis provides many elegant approaches to differential operators and related tools in PDE-based image processing. Our work develops the idea of using a more localized basis than the Fourier one in the context of variational methods based on diffuse interfaces ([14],[5],[6]). Our philosophy involves looking for new types of pseudo-differential energy functionals, that inherit important properties of classical functionals, but leave out the computational drawbacks associated with the discrete differentiation.

Wavelets appeared in the variational context in a number of works ([8], [12] and more). We use a well-known characterization of function regularity in terms of the wavelet coefficients, we also take a widely used PDE -based functional to become a prototype of the new energy we design. However, our approach is conceptually different from the wavelet-PDE techniques that use wavelets to solve PDEs numerically [4],[11] as well as those involving differentiation in the wavelet domain [9]. The energy functional we study is entirely “derivative-free” as it is defined, nevertheless, it exhibits behavior analogous to the ones of energies used in material science and fluid dynamics.

In classical fluid models, an interface between two fluids is treated as infinitely thin and sharp, and is endowed with properties such as surface tension. Diffuse-interface theories replace this sharp interface with continuous variations of an order parameter, such as density, in a way consistent with microscopic theories of the interface. In the inhomogeneous systems which involve domains of well-defined phases separated by a distinct interface, the diffuse-interface description assumes the smoothness of the transition between phases and approaches the sharp interface model asymptotically. At the same time, if used in signal processing applications, diffuse interface models tend to produce results that are oversmoothed comparing to the optimal output [7]. The Ginzburg-Landau energy

$$GL_\epsilon(f) = \frac{\epsilon}{2} \int |\nabla f(x)|^2 dx + \frac{1}{4\epsilon} \int W(f(x)) dx, \quad W(f) = (f^2 - 1)^2 \quad (dGL)$$

is used in modeling of a vast variety of phenomena including the second-order phase transitions. The wavelet Ginzburg-Landau energy that was introduced in [13], is defined as

$$WGL_\epsilon(f) = \frac{\epsilon}{2} |f|_B^2 + \frac{1}{4\epsilon} \int W(f(x)) dx, \quad f \in H^1, \quad (dWGL)$$

where  $|u|_B$  is a Besov or Besov-type seminorm (described further in 2.1.1), and has a similar diffusive nature. It also approaches its sharp-interface limit (provided the above seminorm is defined via a regular compactly supported wavelet) in a similar manner as the classical Ginzburg-Landau energy.

However, the ways in which the minimizers of WGL and those of GL converge to their sharp limits are different. The classical GL energy produces minimizers with smooth transitions between two steady states, where the sharpness/smoothness of such transitions is determined by the interface width parameter  $\epsilon$ . Wavelet based functionals are inherently multiscale and take advantage of simultaneous space and frequency localization, thus allowing much sharper transitions for the same values of the interface parameter  $\epsilon$  and, at the same time, retaining the regularity of minimizers. This phenomenon is partially produced by the translation-invariant dyadic wavelet transform ([20],[10]) used in the WGL energy design to define the  $B$ -seminorm.

The WGL energy has been shown to have properties easily utilizable in image processing due to the properties of its minimizers to have relatively narrow interface for comparatively large values of  $\epsilon$  ([13],[7]). As an illustration, let us consider the problem of minimizing the following energy:

$$E(u) = WGL(u) + \mu \|u - f\|_{L^2(\Omega)}^2. \quad (\text{InpWGL})$$

It is a reformulation of the WGL minimization under the constraint  $u(x) = f(x), x \in \Omega$ , which represents a typical problem setting for the variational inpainting. This model's design focuses on operating with binary functions, while the problem of image inpainting clearly involves grayscale or color images. Therefore, the above variational problem applies to each bit of the image separately. Fig. 1 shows the given image  $f$  with significant part missing (a) and the final output (b), synthesized from the minimizers of (InpWGL) for every bit.

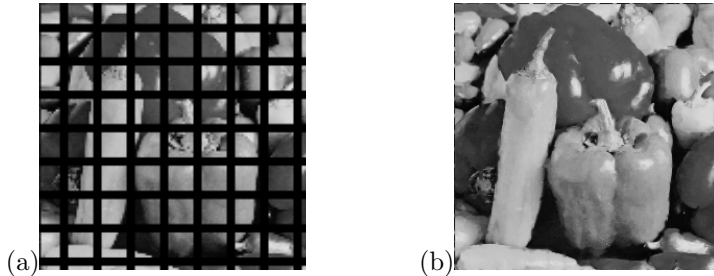


Figure 1: (a) Grayscale image occluded by an artificial grid (about 40% of the pixels are lost), (b) output of the WGL-based bitwise inpainting method.

The notion of  $\Gamma$ -convergence was introduced by E. De Giorgi and T. Franzoni in [18], where it was designed primarily as a notion of convergence for variational functionals on function spaces (one can find details in [2]). One of the highly convenient tools provided by  $\Gamma$ -convergence is the fact that minimizers of approximating functionals converge to the minimizer of the limit energy. This, in particular, is true for diffuse interface problems that converge to the sharp-interface ones as the diffuse interface parameter decreases: for instance, the classical Ginzburg Landau energy converges in the  $\Gamma$ -sense to the Total Variation seminorm, as was shown by Modica and Mortola in [24]. The respective minimizers evolve from  $H^1$ -regular to piecewise constant functions, thus reducing the interface width to zero. Another well known and extensively used example of  $\Gamma$  convergence is the approximation of the jump-dependent Mumford-Shah functional by elliptic functionals defined on Sobolev spaces described in [3]. Again, the  $H^1$  minimizers of the approximating functionals converge to the piecewise-regular minimizers of the approximated energy. Both of the above variational approximations give certain advantages in numerical handling of the related energy minimization problems and were used in image processing applications, such as segmentation, inpainting and more [21], [15], [16], etc.

The modified Ginzburg-Landau functional we introduce in this paper is wavelet-based, however, it inherits many intrinsic properties of energies associated with diffuse interface models. We also prove the convergence of the Wavelet Ginzburg-Landau energy to a bounded multiple of the TV seminorm (a weighted TV seminorm) evaluated on the characteristic functions of sets with finite perimeter. In the general form it can be stated as the following theorem.

**Theorem 1.1** *Let  $\psi$  be an  $r$ -regular ( $r \geq 2$ ) compactly supported wavelet and let  $|\cdot|_B$  denote the associated Besov seminorm in  $\mathbb{R}^N$ . Extend the definition of the WGL energy to all BV functions by setting  $WGL_\epsilon(u) = \infty$  whenever  $u \notin H^1$ . Then*

(a)

$$WGL_\epsilon(u_\epsilon) \xrightarrow{\Gamma} G_\infty(u), \quad G_\infty(u) = \frac{\sqrt{2}}{3} C(u) |u|_{TV},$$

as  $\epsilon \rightarrow 0$  with respect to the  $L_1$  convergence  $u_\epsilon \rightarrow u$ ,  $u_\epsilon \in H^1$  on the set of characteristic functions  $u = \chi_E$  of finite perimeter sets  $E \subset \mathbb{R}^N$ . The variable coefficient  $C(u)$  is a limiting value of the  $H^1 - B$  seminorm ratio associated with the function  $u$ :

$$C(u) = \lim_{n \rightarrow \infty} \frac{|u_n|_B}{|u_n|_{H^1}} \text{ for any sequence } \{u_n\} \subset H^1, \text{ s.t. } u_n \xrightarrow{L_1} u.$$

(b) The limiting energy  $G_\infty$  has the following form:

$$G_\infty(\chi_E) = \int_{\partial E} \rho(\vec{n}(x), \psi) dl(x),$$

where  $\vec{n}(x)$  is the normal to  $\partial E$  at a point  $x$ ,  $\psi$  is a wavelet used to define the  $B$ -seminorm and  $\rho$  is a positive "density" function that depends on  $\vec{n}$ ,  $\psi$  and  $N$  (space dimension).

(c) For every sequence  $\{u_\epsilon\}$  such that not only  $u_\epsilon \rightarrow u$  but also  $|u_\epsilon|_{TV} \rightarrow |u|_{TV}$ , the regular convergence takes place:

$$WGL_\epsilon(u_\epsilon) \rightarrow G_\infty(u) \text{ as } \epsilon \rightarrow 0.$$

Thus, in all dimensions, the classical surface tension model is recovered. An explicit, 1D complexity formula for  $\rho$  in the case  $N = 2$  is derived in Section 3.3.3.

Our result is partially related to the one proven in [1], where the authors also consider a non-local anisotropic energy model involving the double-well potential. However, the non-local part of energy functionals in their study differs from the non-local component of WGL, namely - the Besov seminorm. The differences can be clearly seen in the respective integral operators as well as in the scaling with respect to a decreasing positive parameter. Our proof has certain geometric elements and uses advantages of the wavelet localization.

After proving the main  $\Gamma$ -convergence result we establish the general form of the limiting functional and express it as a function of the wavelet defining the  $B$  seminorm. The limiting functional, acting on the characteristic functions of sets with finite perimeter, is anisotropic and matches the role of the surface tension energy in the Wulff problem [26]. Numerical simulations confirm that the WGL minimizers converge to the minimizers of the respective Wulff problem that were computed as the convex inner envelope of the energy graph in polar coordinates.

## 2 WGL energy in a regular wavelet basis

This section proves the general theorem about the  $\Gamma$ -convergence of WGL energy on the set of characteristic functions of finite perimeter sets. The proof, essentially, consists of two steps. First, we establish the relation between the WGL energy and the TV functional, using the classical result of  $\Gamma$ -convergence and the equivalency relation between the  $H^1$  and Besov seminorms. In this manner, we obtain a sufficient condition for the  $\Gamma$ -convergence of the WGL energy to a multiple of the TV seminorm. It suffices to prove that the  $H^1 - B$  ratio can be extended to the set of characteristic functions of finite perimeter sets by its continuity w.r.t. the  $L_1$  convergence. Namely, any function of the form  $u = \chi_E$ , where  $E \subset \mathbb{R}^N$  has finite perimeter, should have an associated value  $\mathfrak{R}(u)$  such that for any sequence  $u_n \xrightarrow{L_1} u$ ,  $\{u_n\} \subset H^1$

$$\mathfrak{R}(u) = \lim_{n \rightarrow \infty} \frac{|u_n|_B}{|u_n|_{H^1}}.$$

The second part of the proof demonstrates that such extension of the  $H^1 - B$  ratio exists and is a well-defined function, thus establishing the  $\Gamma$ -convergence. We also remark on the  $\Gamma$ -limit of WGL being, in fact, a weighted TV functional and describe the source of the weighting function - a positive density distributed over the set boundary.

## 2.1 WGL and GL energy functionals

### 2.1.1 Definitions and facts

#### CONVENTIONS

The sign of scalar product  $\langle \cdot, \cdot \rangle$  always denotes the one of  $L_2$ .

All wavelet functions we consider are, by default, compactly supported. We also assume those are sufficiently regular for the  $B_{2,2}^1$  (Besov 1-2-2) space to be equivalent to  $H^1$ . Namely, we additionally require that  $\psi$  belongs to  $C^2$  and has  $m \geq 2$  vanishing moments ([20],[23]).

Consider an orthonormal wavelet  $\psi$  and its scaling function  $\phi$ . Define the wavelet mode  $(j, k)$  as

$$\psi_{j,k}(x) = 2^{Nj/2} \psi(2^j x - k), \quad j = 0, 1, 2, \dots, k \in \mathbb{R}^N,$$

and the wavelet transform of a function  $f \in L_2$  at the mode  $(j, k)$  as

$$Wf(j, k) = \langle f, \psi_{j,k} \rangle.$$

Similarly, let us also denote

$$\phi_{j,k}(x) = 2^{Nj/2} \phi(2^j x - k), \quad j = 0, 1, 2, \dots, k \in \mathbb{R}^N.$$

When discussing multi-dimensional cases, we use  $\psi$  as a general notation for the wavelet functions, assuming, wherever needed, summation over all of those. From now on we will be using the *semi-continuous dyadic wavelet transform* ([20]), which produces the following decomposition for any function  $u \in L_2$ :

$$u(x) = \int \langle u, \phi_{0,\mu} \rangle \phi_{0,\mu} d\mu + \sum_j \int \langle u, \psi_{j,\mu} \rangle \psi_{j,\mu} d\mu. \quad (IWT)$$

We will also use the following notation for the continuous analogues of projections of an arbitrary function  $u \in L_2$  on the wavelet-generated ‘‘approximation’’ or ‘‘detail’’ subspaces  $V_j$  or  $W_j$  (as defined in [25]):

$$P_{W_j} u = \int \langle u, \psi_{j,\mu} \rangle \psi_{j,\mu} d\mu,$$

$$P_{V_j} u = \int \langle u, \phi_{0,\mu} \rangle \phi_{0,\mu} d\mu + \sum_{s=0}^{j-1} P_{W_s} u.$$

Whenever we consider functions on finite rectangular domains we will also, without further adjustment of notations, assume that the wavelet transform is periodized (details of this procedure can be found in [20] or [25]). Furthermore, while working with compactly supported functions within the chosen finite domain, one can assume that the periodization of the wavelet transform does not introduce any specifics related to the exceptional behaviour at the domain boundary.

NOTATION Expressions of the form  $X_{W_j}$  or  $X_{V_0}$ , where  $X$  is a normed space ( $L^2$  or  $H^1$ ), when used in the norm (or seminorm) index imply the following evaluation of the norm (or seminorm):

$$\|u\|_{X_{W_j}} = \|\langle u, \psi_{j,\kappa} \rangle\|_X = \|Wu(j, \kappa)\|_X,$$

$$\|u\|_{X_{V_0}} = \|\langle u, \phi_{0,\kappa} \rangle\|_X,$$

where  $\kappa$  is the variable with respect to which the norm is taken, and, analogously,‘

$$|u|_{X_{W_j}} = |\langle u, \psi_{j,\kappa} \rangle|_X, \quad |u|_{X_{V_0}} = |\langle u, \phi_{0,\kappa} \rangle|_X.$$

#### NOTATION

$$a(n) \asymp b(n) \text{ as } n \rightarrow n_0$$

will be used as a short notation for

$$\lim_{n \rightarrow n_0} \frac{a(n)}{b(n)} = 1.$$

DEFINITION For any function  $u \in L_2$  define its  $B$ -seminorm in the discrete form as

$$|u|_{B,d} = \left( \sum_{j=0}^{\infty} 2^{2j} \sum_k |\langle \psi_{j,k}, u \rangle|^2 \right)^{1/2},$$

or, alternatively, in the translation-invariant form:

$$|u|_{B,t.i.} = \left( \sum_{j=0}^{+\infty} 2^{2j} \int |\langle u, \psi_{j,\mu} \rangle|^2 d\mu \right)^{1/2}.$$

These seminorms are evidently equivalent and, according to the above convention, we will be using the translation-invariant form only, naming it  $B$ -seminorm for simplicity. Appendix A.3.1 gives additional details on the relation between the discrete and translation invariant B-seminorms.

If  $\psi$  is an  $r$ -regular wavelet,  $r \geq 2$ , the B-seminorm coincides with the Besov 1-2-2 ( $B_{2,2}^1$ ) seminorm and is equivalent to the  $H^1$  seminorm on the space  $H^1([0, 1]^N)$  (see Appendix A.2 the seminorm definition in case of the unbounded domain). In this paper we consider only  $r$ -regular wavelets with  $r \geq 2$ .

NOTATION We will use  $B$  as an abbreviation for the set of all functions  $u$  for which the  $B$ -seminorm is finite endowed with the corresponding norm  $\|u\|_B = \sqrt{|u|_B^2 + \|u\|_{L_2}^2}$ . In other words,  $B$  will denote the Besov  $B_{2,2}^1$  or an analogous Besov-type space depending on the wavelet we choose to generate the  $B$ -seminorm.

DEFINITION For any function  $u \in H^1$  and define its  $H^1 - B$  ratio to be

$$\mathfrak{R}(u) = \frac{|u|_B}{|u|_{H^1}},$$

where  $B$  is a Besov seminorm generated by an  $r$ -regular,  $r \geq 2$  orthonormal wavelet  $\psi$ .

DEFINITION ( $\Gamma$ -convergence) A family of functionals  $\{F_\epsilon\}$  on a space  $X$  converges to a functional  $F$  in the  $\Gamma$  sense as  $\epsilon \rightarrow 0$  if the following requirements hold:

(i) there exists  $\{u_n\}$ ,  $\epsilon_n$ ,  $u_n \rightarrow u$ , such that

$$\limsup_n F_{\epsilon_n}(u_n) \leq F(u),$$

(ii) for any sequence  $\epsilon_n \rightarrow 0$ , function  $g$  and function sequence  $g_n \rightarrow g$  in  $X$

$$F(g) \leq \liminf_n F_{\epsilon_n}(g_n).$$

An important fact: global minimizers of  $F_\epsilon$  converge to global minimizers of  $F$  ( for details see [22],[17]).

**Lemma 2.1** ( A classical result of  $\Gamma$ -convergence [24], details of which are discussed in [19]).

Define a generalization of the GL functional on the set of BV functions:

$$GL_\epsilon^*(u) = \begin{cases} GL_\epsilon(u), & u \in H^1, \\ +\infty, & u \in BV \setminus H^1. \end{cases}$$

Then, as  $\epsilon \rightarrow 0$ ,  $\frac{3}{\sqrt{2}}GL_\epsilon$  converges to the Total Variation functional in the  $\Gamma$  sense as  $\epsilon \rightarrow 0$ .

### 2.1.2 The role of seminorm equivalency in the $\Gamma$ -convergence of the wavelet Ginzburg-Landau energy.

First, we are going to establish relations between the GL and WGL energies that appear due to the respective norm equivalency. Then we restate the problem of establishing the  $\Gamma$ -convergence of WGL so that it takes a more concrete and approachable form. Let  $B$  denote a classical Besov space  $B_{2,2}^1$  with a norm generated by an  $r$ -regular wavelet  $\psi$ .

Now we will compare the regular and wavelet Ginzburg-Landau energies using the equivalency of the respective seminorms:

$$a|u|_{H^1} \leq |u|_B \leq b|u|_{H^1}.$$

The constants  $a$  and  $b$  depend on the wavelet  $\psi$ . Some remarks about the seminorm equivalency can be found in Appendix A.2.

Substituting the above estimates in the definition of WGL implies

$$\frac{a^2\epsilon}{2} \int |\nabla u|^2 dx + \frac{1}{4\epsilon} \int W(u) dx \leq WGL_\epsilon(u) \leq \frac{b^2\epsilon}{2} \int |\nabla u|^2 dx + \frac{1}{4\epsilon} \int W(u) dx.$$

We will use variable rescaling to investigate the asymptotical behavior of the WGL functional. Let  $\epsilon_a = a^2\epsilon$ ,  $\epsilon_B = b^2\epsilon$ ,  $u_a(x) = u(x/a)$ ,  $u_b(x) = u(x/b)$ , then

$$\begin{aligned} \frac{a^2\epsilon}{2} \int |\nabla u|^2 dx + \frac{1}{4\epsilon} \int W(u) dx &= \frac{\epsilon_a}{2} \int |\nabla u|^2 dx + \frac{a^2}{4\epsilon_a} \int W(u) dx = \\ &= \frac{\epsilon_a}{2} \int |\nabla u_a|^2 dx + \frac{1}{4\epsilon_a} \int W(u_a) dx = GL_{\epsilon_a}(u_a). \end{aligned}$$

An analogous statement is true for  $\epsilon_b$  and  $u_b$ , so

$$GL_{\epsilon_a}(u_a) \leq WGL_\epsilon(u) \leq GL_{\epsilon_b}(u_b).$$

For any sequence  $v^{(\epsilon)} \rightarrow u$ ,

$$\liminf_{\epsilon_a} GL_{\epsilon_a}(v_a^{(\epsilon)}) \geq \frac{\sqrt{2}a}{3} \int |\nabla(u(x))| dx,$$

hence,

$$\liminf_{\epsilon} WGL_\epsilon(v^{(\epsilon)}) \geq \frac{\sqrt{2}a}{3} \int |\nabla(u(x))| dx. \quad (L)$$

There exists a sequence  $u^{(\epsilon)} \rightarrow u$  such that

$$\limsup_{\epsilon_b} GL_{\epsilon_b}(u_b^{(\epsilon)}) \leq \frac{\sqrt{2}b}{3} \int |\nabla(u(x))| dx.$$

Then this sequence also satisfies

$$\limsup_{\epsilon} WGL_\epsilon(u^{(\epsilon)}) \leq \frac{\sqrt{2}b}{3} \int |\nabla(u(x))| dx. \quad (H)$$

Now, if  $u_\epsilon \xrightarrow{L^1} u$ ,  $u_\epsilon \in H^1$  and  $u \in BV \setminus H^1$  then, naturally,  $|u_\epsilon|_{H^1}$  and  $|u_\epsilon|_B$  increase to  $+\infty$ . However, due to the seminorm equivalency, the ratio  $\mathfrak{R}(u_\epsilon)$  stays bounded. The above estimates use the most general values of the equivalency constants  $a$  and  $b$ , which provide the equivalency relation on the entire space. In fact, the argument stays valid after re-assigning:

$$a = \liminf \frac{|u_\epsilon|_B}{|u_\epsilon|_{H^1}}, \quad b = \limsup \frac{|u_\epsilon|_B}{|u_\epsilon|_{H^1}}.$$

This proves the following sufficient condition for the  $\Gamma$  convergence of WGL and explains the origin of statement (a) in Theorem 1.1.

**Lemma 2.2** *Let  $\mathcal{B}$  be a subset of  $BV$  such that for any element  $u \in \mathcal{B}$  and any sequence  $\{u_\epsilon\} \subset H^1$ ,  $u_\epsilon \xrightarrow{L^1} u$  the numerical sequence  $\mathfrak{R}(u_\epsilon)$  converges to the same limit depending on  $u$ . Then WGL functional  $\Gamma$ -converges to a limit defined on  $\mathcal{B}$ .*

An example of a countable set of functions with the same ratio of  $H^1$  and  $B$  seminorms is a wavelet basis generated by a regular wavelet  $\psi$

$$\frac{|\psi_{j,k}|_B}{|\psi_{j,k}|_{H^1}} = \frac{1}{|\psi|_{H^1}}.$$

## 2.2 The $H^1 - B$ ratio defined for characteristic functions of finite perimeter sets in $\mathbb{R}^N$

Let us extend the notion of the  $H^1 - B$  ratio to the set of characteristic functions of finite perimeter sets. By proving that this value exists and is well-defined we will show that part (a) of Theorem 1.1 holds true. For any  $u = \chi_E$ , where  $E \subset \mathbb{R}^N$  is a finite perimeter set ( $|\partial E| < \infty$ ) define its  $H^1 - B$ -ratio  $\mathfrak{R}(u)$  as a limit of such ratios of its wavelet decomposition's partial sums, provided this limit exists:

$$\mathfrak{R}(u) = \lim_{J \rightarrow \infty} \mathfrak{R}(u_J) = \lim_{J \rightarrow \infty} \frac{|u_J|_{H^1}}{|u_J|_B}, \quad u_J = \sum_{j=0}^J \int \langle u, \psi_{j,\kappa} \rangle \psi_{j,\kappa} d\kappa.$$

Now we will prove that the above limit exists and coincides with such limit of any sequence of functions in  $H^1$  approximating  $u$  in the  $L_1$  sense.

### 2.2.1 Characteristic function of a hyperplane in $\mathbb{R}^N$ and its wavelet domain restriction to $[0, 1]^N$

In order to prove that the  $H^1 - B$  ratios of partial sums of the above wavelet series representing a characteristic function  $u = \chi_E$ , converge, we explore the relation between the projections of the characteristic function on consecutive wavelet scales. Based on this, we conclude the proof by showing that  $B$  and  $H^1$  seminorms of respective partial wavelet sums grow asymptotically as constant multiples of  $2^{J/2}$ , where  $J$  is the maximum wavelet scale in the partial sum.

REMARK The partial wavelet sums  $u_J$  converge to the function  $u \in BV \setminus H^1$ , so both  $|u_J|_{H^1}$  and  $|u_J|_B$  seminorms tend to  $\infty$  as  $J \rightarrow \infty$ . Therefore, any finite number of terms in the series is negligible for the purposes of computing the limiting  $H^1 - B$  ratio. In particular, one can disregard the contribution of  $P_{V_0} u$  within  $|u_J|_{H^1}$ ,  $|u_J|_B$  when computing  $\mathfrak{R}(u)$ .

We start from considering a characteristic function of a half-space. Even though it does not belong to  $L^2$ , its formal wavelet decomposition exists: the wavelet transform at every wavelet mode is well-defined since we consider compactly supported wavelet kernel, moreover, the reconstruction formula (IWT) is locally valid.

DEFINITION 1 Let  $\pi$  be a hyperplane in  $\mathbb{R}^N$ . It divides  $\mathbb{R}^N$  in two half-spaces, let  $\chi_\pi$  denote the characteristic function of one of them.

The choice of the half-space is not important since it can only affect the sign of wavelet coefficients of the respective characteristic function, which is negligible since we are going to operate with the squares of those coefficients. This definition is illustrated in Fig.2

**Lemma 2.3** The formal wavelet decomposition of  $\chi_\pi$  has the following special form:

$$\chi_\pi(x) = P_{V_0} \chi_\pi(x) + \sum_{j=0}^{\infty} U(2^j x), \quad U = P_{W_0} \chi_\pi.$$

The wavelet transform of  $\chi_\pi$  is invariant with respect to translations parallel to the hyperplane: if  $\vec{k} - \vec{m}$  is parallel to  $\pi$ , then  $\langle \chi_\pi, \psi_{j,\vec{k}} \rangle = \langle \chi_\pi, \psi_{j,\vec{m}} \rangle$ .

Proof. Let us compute the wavelet transform of  $\chi_\pi$  formally with respect to a compactly supported smooth wavelet  $\psi$ . We use the translation-invariant dyadic wavelet transform, hence, one can assume that the coordinate origin lies on  $\pi$  and hence,  $\chi_\pi$  is homogeneous of degree 0. Then

$$\langle \chi_\pi, \psi_{j,k} \rangle = \int \chi_\pi(x) 2^{Nj/2} \psi(2^j x - k) dx = \int \chi_\pi(x) 2^{-Nj/2} \psi(x - k) dx = 2^{-Nj/2} \langle \chi_\pi, \psi_{0,k} \rangle.$$

Therefore, according to (IWT),  $\chi_\pi$  is written in the needed form. The last part of the statement is implied, again, by the translation invariance of the wavelet transform and the linear structure of  $\chi_\pi$ . It shows, in particular, that the range of the wavelet transform for this function can be obtained by translating the

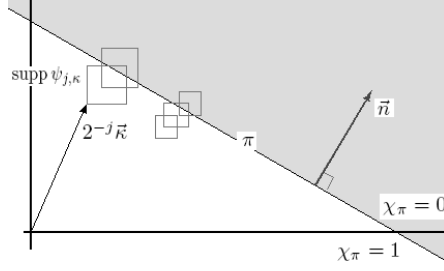


Figure 2: Illustration to the Definition 1 and Lemma 2.3: positions of the compact supports of the dilated and translated wavelet kernels  $\psi_{j,k}$  relative to hyperplane  $\pi$  in  $\mathbb{R}^2$  suggest that wavelet transform values vary only w.r.t. the shifts in the direction of  $\vec{n}$  (normal to the hyperplane).

wavelet kernel along the direction normal to the hyperplane. ■

The following lemma describes properties of the same function within a finite domain, in particular  $[0, 1]^N$ . It is more convenient to consider restrictions of the above function in the wavelet domain with the purpose of preserving the uniformity of the function structure at each wavelet scale. According to the remark in the beginning of this section, we also omit the projection on the subspace  $V_0$  in computations related to the  $H^1 - B$  ratio.

**DEFINITION 2** *Given a hyperplane  $\pi$ , define  $f^\pi$  to be a wavelet-domain restriction of  $\chi_\pi$  to the unit cube, assuming the hyperplane intersects it:*

$$f^\pi(x) = \sum_{j=0}^{\infty} P_{W_j} f^\pi(x), \quad P_{W_j} f^\pi = \int_{\vec{\kappa}: \kappa_i \in [0, 2^j]} \langle \chi_\pi, \psi_{j, \vec{\kappa}} \rangle \psi_{j, \vec{\kappa}} d\kappa$$

and its partial wavelet sums

$$f_J^\pi = \sum_{j=0}^J \int_{\vec{\kappa}: \kappa_i \in [0, 2^j]} \langle \chi_\pi, \psi_{j, \vec{\kappa}} \rangle \psi_{j, \vec{\kappa}} d\kappa.$$

Figure 3 gives an intuitive illustration to the definition and a numerical example. Here instead of the completely self-similar representation as such for the half-space we get the one where each next level has both the variable and the range of translations rescaled, i.e. the same pattern gets  $2^j$  times shrunk in each direction and the same number of times more repeated. As the wavelet scale  $j$  increases

$$|P_{W_j} f(x) - P_{W_j} (\chi_\pi \chi_{[0, 1]^N})|_B = o(|P_{W_j} f(x)|_B)$$

due to the compact localization of wavelets. Indeed, the above difference consists of only those wavelet modes whose supports include points from  $\pi \cap \partial[0, 1]^N$ . The conclusion follows from the fact that the Lebesgue measure of this intersection as a subset of the hyperplane endowed with the  $N - 1$  dimensional Lebesgue measure is zero:  $\mu_{N-1}^\pi(\pi \cap \partial[0, 1]^N) = 0$ .

The following lemma describes the asymptotic behaviour of the  $H^1$  and  $B$  seminorms of  $f_J^\pi$  as  $J \rightarrow \infty$ . Its proof also demonstrates that, for the purposes of computing the  $H^1 - B$  ratio, one can perform the differentiation and integration needed for computing those seminorms in the wavelet domain.

**Lemma 2.4** *Functions  $f_J^\pi$  (as in Definition 2) satisfy:*

$$(a) \|f_J^\pi\|_B^2 \asymp (2^{J+1} - 1) \|f^\pi\|_{L_{W_0}^2}^2$$

$$(b) \|f_J^\pi\|_{H^1}^2 \asymp (2^{J+1} - 1) |f_0^\pi|_{H_{W_0}^1}^2 \quad \text{as } J \rightarrow \infty$$



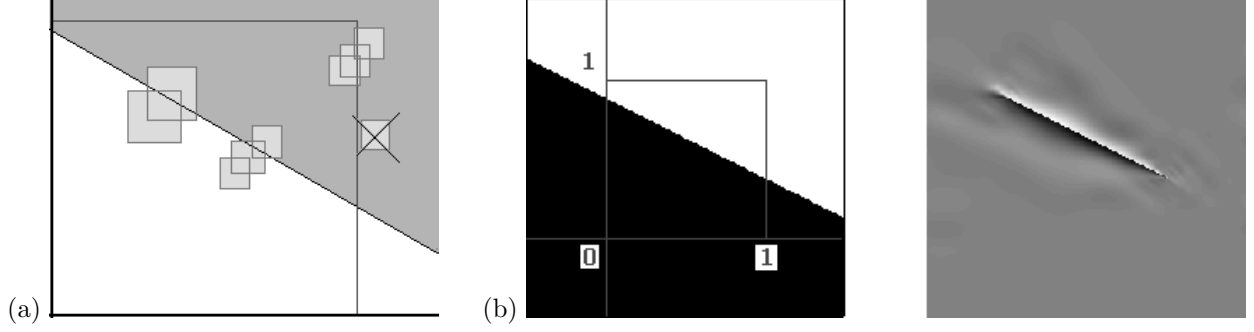


Figure 3: (a) Illustration to the Definition 2: supports of  $\psi_{j,k}$  included and not included in the wavelet domain restriction to the unit square. (b) Computational example: the original characteristic function and its wavelet domain restriction to the unit square (in the case of Daubechies 4 wavelet).

Proof. 1. *Preliminary discussion* An important instrument of this proof is the self-similarity described in Lemma 2.3 applied to a bounded subset of wavelet transform modes that defines  $f^\pi$ :

$$f_J^\pi = \sum_{j=0}^J 2^{-Nj/2} \int \langle f^\pi, \psi_{0,k_n} \rangle \psi_{j,k} dk, \quad (WF - f^\pi)$$

where  $k_n$  is a projection of the translation vector  $k$  on the normal  $n$  to the hyperplane  $\pi$ . Here we disregard the wavelet coefficients near the boundary of  $\text{supp } f^\pi$ , since they do not affect the asymptotical behavior of  $|f^\pi|_B$  or  $|f^\pi|_{H^1}$  (as was remarked after the definition of  $f^\pi$ ). Hence we assume  $\langle f^\pi, \psi_{j,k} \rangle = \langle \chi_\pi, \psi_{j,k} \rangle$  so the proportionality between the coefficients of different levels is preserved.

This proof will also use the following property of the Fourier transforms of the wavelet and its scaling function:

$$|\hat{\phi}(\xi)|^2 + \sum_{j=0}^{\infty} |\hat{\psi}(2^{-j}\xi)|^2 = 1 \text{ for a.e. } \xi \in \mathbb{R}^N.$$

Here the Fourier transform of a function  $f$  is assumed to have the form

$$\hat{f}(\xi) = \int f(x) e^{-2\pi i x \cdot \xi} dx.$$

2. *Main part of the proof* To prove the statements (a) and (b), we are going to define the values that actually coincide with the r.h.s. of the respective relations and then show that those values are asymptotically equivalent to the l.h.s. seminorms. For any function  $u \in \mathbb{R}^N$  let

$$\beta_J(u) = \sum_{j=0}^J 2^{2j} \int \langle u, \psi_{j,\mu} \rangle^2 d\mu$$

$$\zeta_J(u) = \sum_{j=0}^J 2^{2j} \sum_{i=1}^N \int |\partial_{k_i} \langle u, \psi_{j,\mu} \rangle|^2 d\mu.$$

*Proof of (a)* Let us show that  $\beta_J(f^\pi)$  is exactly equal to  $(2^{J+1} - 1) \|f^\pi\|_{L_{W_0}^2}^2$ :

$$\beta_J(f^\pi) = \sum_{j=0}^J \int_{[0, 2^j]^N} 2^{2j} \langle f^\pi, \psi_{j,k} \rangle^2 dk = \sum_{j=0}^J \int_{[0, 1]^N} 2^{2j} \langle f^\pi, \psi_{0,\mu} \rangle^2 d\mu = (2^{J+1} - 1) \|f^\pi\|_{L_{W_0}^2}^2.$$

The statement (a) of this lemma is proven once we show that  $\beta_J(f^\pi)$  is equivalent to the B-seminorm of  $f_J^\pi$  as  $J \rightarrow \infty$ . Indeed, in terms of the Fourier transforms of  $f^\pi$  and  $\psi$ ,

$$\beta_J(f^\pi) = \int |\hat{f}^\pi(\xi)|^2 \sum_{j=0}^J 2^{2j} |\hat{\psi}(2^{-j}\xi)|^2 d\xi,$$

$$|f_J^\pi|_B^2 = \int |\hat{f}^\pi(\xi)|^2 \left( \sum_{j=0}^J |\psi(2^{-j}\xi)|^2 \right)^2 \sum_{j=0}^{\infty} 2^{2j} |\psi(2^{-j}\xi)|^2 d\xi.$$

Let us show that the difference of the above values is  $o(\beta_J(u))$  as  $J \rightarrow \infty$ .

$$\begin{aligned} |\beta_J(f^\pi) - |f_J^\pi|_B^2| &\leq \int |f^\pi(\xi)|^2 \sum_{j=0}^J 2^{2j} |\psi(2^{-j}\xi)|^2 \left( 1 - \left( \sum_{j=0}^J |\psi(2^{-j}\xi)|^2 \right)^2 \right) d\xi + \\ &+ \int |f^\pi(\xi)|^2 \left( \sum_{j=0}^J |\psi(2^{-j}\xi)|^2 \right)^2 \sum_{j=J+1}^{\infty} 2^{2j} |\psi(2^{-j}\xi)|^2 d\xi \leq \\ &2 \int |f^\pi(\xi)|^2 \sum_{j=0}^J 2^{2j} |\psi(2^{-j}\xi)|^2 (|\hat{\phi}(\xi)|^2 + \sum_{j=J+1}^{\infty} |\psi(2^{-j}\xi)|^2) d\xi + \\ &+ \int |f^\pi(\xi)|^2 \left( \sum_{j=0}^J |\psi(2^{-j}\xi)|^2 \right)^2 \sum_{j=J+1}^{\infty} 2^{2j} |\psi(2^{-j}\xi)|^2 d\xi. \end{aligned}$$

Now, recall that we assumed  $\psi$  to be  $r$ -regular with  $r \geq 2$ , so  $\psi \in H^2$ ,  $\Delta_w \psi \in L^2(\mathbb{R}^N)$ . Also, since  $\psi$  is compactly supported, so is  $\Delta_w \psi$ , hence,  $\widehat{\Delta_w \psi} \in C(\mathbb{R}^N) \cap L^2(\mathbb{R}^N)$  and thus  $\widehat{\Delta_w \psi} \in L^\infty(\mathbb{R}^N)$ . Therefore,

$$\hat{\psi}(\xi) \overline{\widehat{\Delta_w \psi}} = |\hat{\psi}(\xi)|^2 \sum_{j=0}^{\infty} 2^{2j} |\hat{\psi}(2^{-j}\xi)|^2 \in L^\infty(\mathbb{R}^N).$$

An analogous statement is true for the scaling function  $\phi$ . Therefore, we obtain

$$\begin{aligned} \int |f^\pi(\xi)|^2 \sum_{j=0}^J 2^{2j} |\psi(2^{-j}\xi)|^2 |\hat{\phi}(\xi)|^2 d\xi &\leq \|\hat{\phi}\|_{L^\infty} \|\widehat{\Delta_w \phi}\|_{L^\infty} \|f^\pi\|_{L^2}^2, \\ \int |f^\pi(\xi)|^2 \sum_{j=0}^J 2^{2j} |\psi(2^{-j}\xi)|^2 \sum_{j=J+1}^{\infty} |\psi(2^{-j}\xi)|^2 d\xi &\leq \int |f^\pi(\xi)|^2 \left( \sum_{j=0}^J |\psi(2^{-j}\xi)|^2 \right)^2 \sum_{j=J+1}^{\infty} 2^{2j} |\psi(2^{-j}\xi)|^2 d\xi, \\ \int |f^\pi(\xi)|^2 \left( \sum_{j=0}^J |\psi(2^{-j}\xi)|^2 \right)^2 \sum_{j=J+1}^{\infty} 2^{2j} |\psi(2^{-j}\xi)|^2 d\xi &\leq (J+1) \|\hat{\psi}\|_{L^\infty} \|\widehat{\Delta_w \psi}\|_{L^\infty} \|f^\pi\|_{L^2}^2. \end{aligned}$$

Hence, the entire expression estimating  $|\beta_J(f^\pi) - |f_J^\pi|_B^2|$  from above is bounded by a function of order  $O(J)$  as  $J \rightarrow \infty$ , while  $\beta_J(u) = O(2^J)$ . So,  $\beta_J(f^\pi) = (2^{J+1} - 1) \|f^\pi\|_{L_{W_0}^2}^2 \asymp |f_J^\pi|_B^2$ , i.e. the statement (a) is proven.

*Proof of (b)* We prove statement (b) using the same strategy. Evaluation of  $\zeta_J(f^\pi)$  with respect to  $(WF - f^\pi)$  shows that it equals to the r.h.s. of relation (b):

$$\begin{aligned} \zeta_J(f^\pi) &= \sum_{j=0}^J 2^{2j} \sum_{i=1}^N \int_{k \in [0, 2^j]^N} 2^{-Nj} |\partial_{k_i} \langle f^\pi, \psi_{0,k} \rangle|^2 dk = \\ &\sum_{j=0}^J 2^j \sum_{i=1}^N \int_{k \in [0, 1]^N} |\partial_{k_i} \langle f^\pi, \psi_{0,k} \rangle|^2 dk = (2^{J+1} - 1) |f^\pi|_{H_{W_0}^1}^2. \end{aligned}$$

To prove that  $\zeta_J(f^\pi)$  is equivalent to  $|f_J^\pi|_{H^1}^2$  we rewrite both expressions in terms of the Fourier transforms:

$$\zeta_J(f^\pi) = \sum_{j=0}^J 2^{2j} \int 4\pi^2 |\xi|^2 |\hat{f}^\pi \xi \hat{\psi}(2^{-j}\xi)|^2 d\xi,$$

$$|f_J^\pi|_{H^1}^2 = \int 4\pi^2 |\xi|^2 |\hat{f}^\pi(\xi)|^2 \left( \sum_{j=0}^J |\hat{\psi}(2^{-j}\xi)|^2 \right) d\xi.$$

Let us estimate the difference:

$$\begin{aligned} \zeta_J(f^\pi) - |f_J^\pi|_{H^1}^2 &= 4\pi^2 \int |\xi|^2 |\hat{f}^\pi(\xi)|^2 \left( \sum_{j=0}^J |\hat{\psi}(2^{-j}\xi)|^2 \right) \left( 1 - \sum_{j=0}^J |\hat{\psi}(2^{-j}\xi)|^2 \right) d\xi = \\ &= 4\pi^2 \int |\xi|^2 |\hat{f}^\pi(\xi)|^2 \left( \sum_{j=0}^J |\hat{\psi}(2^{-j}\xi)|^2 \right) (|\hat{\phi}(\xi)|^2 + \sum_{j=J+1}^{\infty} |\hat{\psi}(2^{-j}\xi)|^2) d\xi \end{aligned}$$

Here both  $\psi, \phi$  and  $\Delta\psi, \Delta\phi$  are continuous and compactly supported, hence,  $\hat{\psi}(\xi), \hat{\phi}(\xi), \xi^2\hat{\psi}(\xi), \xi^2\hat{\phi}(\xi) \in L^\infty(\mathbb{R}^N)$  and

$$\begin{aligned} &\int |\xi|^2 |\hat{f}^\pi(\xi)|^2 |\hat{\phi}(\xi)|^2 d\xi \leq \|\xi\hat{\phi}(\xi)\|_{L^\infty}^2 \|f^\pi(\xi)\|_{L^2}^2, \\ &\int |\xi|^2 |\hat{f}^\pi(\xi)|^2 \sum_{j=0}^J |\hat{\psi}(2^{-j}\xi)|^2 \sum_{j=J+1}^{\infty} |\hat{\psi}(2^{-j}\xi)|^2 d\xi \leq \\ &\leq \|\widehat{\Delta\psi}\| \int |\hat{f}^\pi(\xi)|^2 \sum_{j=0}^J 2^{2j} |\hat{\psi}(2^{-j}\xi)|^2 \sum_{j=J+1}^{\infty} |\hat{\psi}(2^{-j}\xi)|^2 d\xi \leq J \|\widehat{\Delta\psi}\|_{L^\infty} \|\widehat{\Delta_w\psi}\|_{L^\infty} \|f^\pi\|_{L^2}^2 \\ &|\zeta_J(f^\pi) - |f_J^\pi|_{H^1}^2| \leq O(1) + O(J), \quad |\zeta_J(f^\pi) - |f_J^\pi|_{H^1}^2| / \zeta_J(f^\pi) \rightarrow 0, \quad J \rightarrow \infty \end{aligned}$$

Hence,  $\zeta_J(f^\pi) = (2^{J+1} - 1) |f^\pi|_{H_{W_0}^1} \asymp |f_J^\pi|_{H^1}^2$ . ■

**COROLLARY 1** (from lemma 2.4) *There exist functions  $\rho_B$  and  $\rho_{H^1}$  such that for any hyperplane  $\pi$  with normal vector  $\vec{n}_\pi$*

$$|f_J^\pi|_{H^1}^2 \asymp 2^J s_\pi (\rho_{H^1})^2 (\vec{n}_\pi), \quad |f_J^\pi|_B^2 \asymp 2^J s_\pi (\rho_B)^2 (\vec{n}_\pi),$$

where  $s_\pi$  is the  $n - 1$ -dimensional measure of the part of the hyperplane inside of the unit cube.

*Proof.* Due to the translation invariancy, functions  $f^{\pi'}$ , associated with all hyperplanes  $\pi'$  parallel to  $\pi$  and intersecting the unit cube, have the same structure of wavelet decomposition up to a shift in indices. By lemma 2.3 the values of the wavelet transform repeat along the hyperplane, while the total amount of the repeating values  $Wf^{\pi'}(0, k)$  is proportional to the area of the hyperplane enclosed within the unit cube. ■

Using lemma 2.4 and its corollary, we can define the values  $\rho_B$  and  $\rho_{H^1}$  as explicit functions of the normal to the respective hyperplane.

**DEFINITION 3** *Take an arbitrary hyperplane  $\pi$  with a normal vector  $\vec{n}$  that intersects the unit cube  $[0, 1]^N$  non-trivially, let the area (the  $N - 1$  dimensional measure defined on the hyperplane) of the crosssection equal  $s$ . Restricting the wavelet indices in the same manner as in definition 2, define:*

$$\begin{aligned} \rho_B(\vec{n}) &= s^{-1/2} |f^\pi|_{L_{W_0}^2} = s^{-1/2} \left[ \sum_{j=0}^J \int_{\kappa: 0 \leq \kappa_i \leq 1} |\langle \chi_\pi, \psi_{0,\kappa} \rangle|^2 d\kappa \right]^{1/2}, \\ \rho_{H^1}(\vec{n}) &= s^{-1/2} |f^\pi|_{H_{W_0}^1} = s^{-1/2} \left[ \sum_{i=1}^N \int_{\kappa: 0 \leq \kappa_i \leq 1} |\partial_{\kappa_i} \langle f^\pi, \psi_{j,\kappa} \rangle|^2 d\kappa \right]^{1/2}. \end{aligned}$$

**COROLLARY 2** (from lemma 2.4) *Consider a function  $u$  that is a restriction of some  $\chi_\pi(x)$  to  $[0, 1]^N$  either spatially or in the modes of its wavelet transform. Then the  $H^1 - B$  ratio of  $u$  exists and has the form*

$$\mathfrak{R}(u) = \frac{|f^\pi|_{L_{W_0}^2}}{|f^\pi|_{H_{W_0}^1}}.$$

Next step is to consider a polyhedral set  $P$  in  $\mathbb{R}^N$  and apply the relations derived above to each of its faces.

### 2.2.2 $H^1 - B$ ratio of characteristic functions of polyhedra generalized for all finite perimeter sets

Consider a polyhedron  $P \subset \mathbb{R}^N$  with  $M$  faces  $F_i$ ,  $i = 1, \dots, M$ . Let  $\pi(F_i), i = 1, \dots, M$  denote the hyperplanes containing respective faces and let  $u = \chi_P$ .

**Lemma 2.5** The  $H^1 - B$  ratio of  $u = \chi_E$ , where  $E \subset \mathbb{R}^N$  is a polyhedron, satisfies

$$\mathfrak{R}(u)^2 = \lim_{j \rightarrow \infty} \frac{\sum_i |f_j^{\pi(F_i)}|_{H^1}^2}{\sum_i |f_j^{\pi(F_i)}|_B^2} = \lim_{j \rightarrow \infty} \frac{\sum_i (\rho_B)^2 (n(F_i)) |F_i|}{\sum_i (\rho_{H^1})^2 (n(F_i)) |F_i|},$$

where  $n(F_i)$  denotes the normal to the face  $F_i$  and  $\pi(F_i)$  - the hyperplane through  $F_i$ .

Proof. Let us estimate the difference

$$\left| \sum_{j=0}^J P_{W_j} u|_B^2 - \sum_i |f_j^{\pi(F_i)}|_B^2 |F_i|^2 \right|.$$

To simplify the discussion, let  $u^{(F_i)}$  denote the wavelet domain restriction of function  $u$  to the polyhedral face  $F_i$ :

$$u^{(F_i)}(x) = \sum_{j=0}^{\infty} \int_{k \in K(F_i, j)} \langle u, \psi_{j,k} \rangle \psi_{j,k}(x) dk, \quad K(F_i, j) = \{k : \text{supp } \psi(2^j x - k) \cap F_r = \emptyset, r \neq i\}.$$

We also notice that the wavelet transform of any characteristic function is uniformly bounded:

$$|\langle \chi_{E'}, \psi_{j,k} \rangle| \leq 2^{-Nj/2} C, \quad C = \max_{\Omega \subset \mathbb{R}^N} \int_{\Omega} \psi(x) dx.$$

By construction, the difference between the partial wavelet sums  $\sum_{j=0}^J P_{W_j} u$  and the partial wavelet sums of auxiliary functions  $\sum_i \sum_{j=0}^J P_{W_j} u^{(F_i)}$  can possibly have non-zero wavelet transform only at the modes  $j, k$  such that  $\text{supp } \psi_{j,k}$  intersects  $\cup_i \partial F_i$ . Therefore, the Sobolev and Besov seminorms of this difference can be majorized (up to a constant multiple) by the product of the coefficient upper bound squared and the measure of all wavelet mode indices relevant to the polyhedron edges:

$$\left| \sum_{j=0}^J P_{W_j} u - \sum_i f_J^{\pi(F_i)} \right|_B^2 \leq C' \sum_{j=0}^J 2^{2j} 2^{-Nj} 2^{(N-2)j} = C' J.$$

Here  $C'$  depends, besides  $C$ , on the total length of all polyherdal edges, the size of the wavelet support and the space dimension  $N$ .

Furthermore, one observes that  $\sum_{j=0}^J P_{W_j} u^{(F_i)}$  has the structure analogous to the one of  $f_J^{\pi(F_i)}$ , only with the set of wavelet modes restricted to those in a neighborhood of the polyhedral face  $F_i$  rather than to the modes inside the unit cube. Hence, by a similar argument,

$$\left| \sum_{j=0}^J P_{W_j} u^{(F_i)} \right|_B^2 - |f_J^{\pi(F_i)}|_B^2 |F_i|^2 \leq C'' J.$$

Finally, we achieve:

$$\left| \sum_{j=0}^J P_{W_j} u|_B^2 - \sum_i |f_j^{\pi(F_i)}|_B^2 |F_i|^2 \right| \leq \left| \sum_{j=0}^J P_{W_j} u - \sum_i f_J^{\pi(F_i)} \right|_B^2 + \sum_i \left| \sum_{j=0}^J P_{W_j} u^{(F_i)} \right|_B^2 - |f_J^{\pi(F_i)}|_B^2 |F_i|^2 \leq O(J).$$

This, together with lemma 2.4, conclude the proof of the first equality. The second equality follows from the first by the Corollary from Lemma 2.4. ■

The next statement establishes that the  $H^1 - B$  ratio  $\mathfrak{R}$  is a well-defined function on the set of characteristic functions of finite perimeter sets.

**Lemma 2.6** Let  $u_n \rightarrow u$  in  $L^1$ , where  $u \notin H^1$ . Denote  $u_J = P_{V_J}u$  and  $u_J^n = P_{V_J}u^n$ . Then

$$\left| \frac{|u_J^n|_{H^1}}{|u_J^n|_B} - \frac{|u_J|_{H^1}}{|u_J|_B} \right| \leq O(\|u - u_n\|_{L^2}).$$

Since the estimate is independent of the scale  $J$ ,  $\mathfrak{R}(u)$  can be defined via any sequence  $f_n \rightarrow u$  in  $L^2$ :

$$\mathfrak{R}(u) = \lim_{n \rightarrow \infty} \frac{|P_{V_n}f_n|_{H^1}}{|P_{V_n}f_n|_B} \text{ or } \mathfrak{R}(u) = \lim_{n \rightarrow \infty} \mathfrak{R}(u_n).$$

Proof.

Fix an arbitrary scale  $J$ .

$$\begin{aligned} \left| \frac{|u_J^n|_{H^1}}{|u_J^n|_B} - \frac{|u_J|_{H^1}}{|u_J|_B} \right| &= \left| \frac{(|u_J^n|_{H^1} - |u_J|_{H^1})|u_J^n|_B - (|u_J^n|_B - |u_J|_B)|u_J^n|_{H^1}}{|u_J^n|_B|u_J|_B} \right| \leq \\ & \frac{|u_J^n - u_J|_{H^1}}{|u_J|_B} + \frac{|u_J^n - u_J|_B|u_J^n|_{H^1}}{|u_J^n|_B|u_J|_B} \leq \frac{2|u_J^n - u_J|_B}{a|u_J|_B}, \end{aligned}$$

where  $a$  is the constant from the seminorm equivalency relation  $a|\cdot|_{H^1} \leq |\cdot|_B \leq b|\cdot|_{H^1}$ . Now, since

$$|u_J^n - u_J|_B \leq O(2^J\|u - u_n\|_{L^2}),$$

and, as it was shown earlier,  $|u_J|_B = O(2^J)$ , we conclude

$$\left| \frac{|u_J^n|_{H^1}}{|u_J^n|_B} - \frac{|u_J|_{H^1}}{|u_J|_B} \right| \leq O(\|u - u_n\|_{L^2}).$$

■

**Lemma 2.7** The  $H^1 - B$  ratio exists for any function  $\chi_E$ , where  $E \subset \mathbb{R}^N$  has finite perimeter. It satisfies

$$\mathfrak{R}(\chi_E)^2 = \frac{\int_{\partial E} (\rho_B)^2(n(s))}{\int_{\partial E} (\rho_{H^1})^2(n(s))} ds.$$

Proof.

Let  $P_n$  be a sequence of polyhedra approximating the set  $E$  in the sense of the  $N$ -dimensional Lebesgue measure, i.e.  $\chi_{P_n} \xrightarrow{L^1} \chi_E$ . By lemmas 2.6 and 2.5

$$\mathfrak{R}(u) = \lim_{n \rightarrow \infty} \mathfrak{R}\chi_{P_n} = \lim_{n \rightarrow \infty} \frac{\int_{\partial P_n} (\rho_{H^1})^2(\bar{n}(x)) ds(x)}{\int_{\partial P_n} (\rho_B)^2(\bar{n}(s)) ds(x)},$$

here  $\bar{n}(x)$  denotes the normal to  $\partial P_n$  at the point  $x \in \partial P_n$ . Since the functions  $\rho_B, \rho_{H^1}$  are bounded and continuous (because the projection operator  $P_{W_0}$  is continuous w.r.t. rotations in space, and the densities depend on the 0-th wavelet scale projection only by lemma 2.4), the surface integrals converge uniformly w.r.t.  $n$ . Passing to the limit, we get the needed expression. ■

We have thus proven part (a) of Theorem 1.1. The variable coefficient  $C(u)$  that appears in the statement is indeed the limiting value of the  $H^1 - B$  ratios of the partial wavelet sums of  $u$ . Our next step is to prove part (b) using the fact that the  $H^1 - B$  ratio, despite its integral form, is a local functional.

### 2.2.3 $\Gamma$ -limit of WGL energy as a weighted surface area functional

**Lemma 2.8** *The  $\Gamma$ -limit of the WGL energy at any function  $\chi_E$ , where  $E \subset \mathbb{R}^N$  has finite perimeter, equals*

$$G_\infty = \frac{\sqrt{3}}{2} \mathfrak{R}(\chi_E) |E| = \frac{\sqrt{3}}{2} \int_{\partial E} \frac{\rho_B(n(x))}{\rho_{H^1}(n(x))} ds(x),$$

where  $n(x)$  is a normal to  $\partial E$  at the point  $x \in \partial E$ .

Proof.

1. *Localization* Since the regular Ginzburg-Landau energy is a local functional, the theorem about its  $\Gamma$ -convergence is true independently of the spatial domain of functions in consideration. Since we use the classical result as the main tool in proving the WGL  $\Gamma$ -convergence, we can consider the asymptotic behavior of the WGL energy locally. Indeed, we can do that due to the fact that the wavelet kernels we use are compactly supported and the observation that any finite number of wavelet scales can be excluded from the Besov seminorm in the WGL expression without any impact on the  $\Gamma$ -limit.

2. *Additivity* As discussed above, the  $\Gamma$  - limit of WGL is invariant w.r.t. the exclusion of any finite number of wavelet scales or any set of wavelet modes indexed within a set of measure zero from the Besov seminorm. Therefore, one can locally redefine the  $B$ -seminorm in the WGL expression as

$$|u|_{B(\omega)}^2 = \int_{\Omega} (-\Delta_w)u(x)u(x)dx, \quad \Delta_w^\Omega u = - \sum_{j=0}^{\infty} 2^{2j} \int_{\kappa: \text{supp } \psi_{j,\kappa} \subseteq \Omega} \langle u, \psi_{j,\kappa} \rangle \psi_{j,\kappa} d\kappa,$$

then the entire WGL energy can be viewed as a single integral over the domain of consideration, and, therefore, is additive with respect to any partition of this domain.

3. *True for polyhedra* In particular, this implies that the  $\Gamma$ -limiting energy calculated at some  $\chi_P$ , where  $P$  is a polyhedron with faces  $F_1, \dots, F_M$ , can be also expressed as

$$\mathfrak{R}(u)|u|_{TV} = \sum_i \frac{\rho_B(n(F_i))}{\rho_{H^1}(n(F_i))} |F_i|.$$

An arbitrary set  $E$ , in its turn, can be approximated by a sequence of polyhedra  $P_n$  with perimeters  $|P_n|$  converging to the perimeter of  $E$ . Then  $\frac{\chi_{P_n}}{L_1 \rightarrow \chi_E}, \mathfrak{R}(\chi_{P_n}) \rightarrow \mathfrak{R}(\chi_E)$ . Letting  $n \rightarrow \infty$  can be viewed as an infinite refinement of the domain partition and leads to the required expression for the  $\Gamma$ -limit. ■

The last part of Theorem 1.1 - statement (c) - is implied by the following argument. As we proved in Lemma 2.6, the  $L_1$  convergence of functions is sufficient for the convergence of the respective  $H^1 - B$  ratios. However, it does not imply the convergence of TV seminorm values. One can obtain an analogous statement about the pointwise limit by making the theorem conditions stronger, i.e. requiring the TV seminorms to converge as well.

## 3 The $\Gamma$ - convergence of the wavelet Ginzburg-Landau energy to the weighted Total Variation functional in one and two space dimensions

This section describes the WGL energy and the  $\Gamma$ -limiting functional defined on functions of one and two variables. The distinguishing feature of the one-dimensional case is the fact that the WGL converges to a constant multiple of TV, since characteristic functions of sets in  $\mathbb{R}^1$  have degenerate boundary. Two-dimensional case is relatively easy to visualize and implement numerically. We assume that the compactly supported wavelet functions in two dimensions are obtained as separable products of one dimensional wavelet and scaling functions. It is the simplest case that can be considered for numerical implementation supporting the theorem proven in the previous section. In both cases, the limiting functional is expressed as a function of the wavelet associated with the  $B$  seminorm used in the WGL definition. In 2D it is naturally anisotropic and matches the role of the surface tension energy in the Wulff problem.

All sets considered in this chapter are bounded, therefore, can be considered as subsets of the unit interval or square in one and two dimensions respectively.

### 3.1 $H^1 - B$ ratio of the step function in 1D.

Consider a step function  $S(x) = -\chi_{x>0} + \chi_{x<0}$ . Notice that  $S - P_{V_0}S$  has compact support.

**Lemma 3.1** The wavelet decomposition of a step function  $S(x) = -\chi_{x>0} + \chi_{x<0}$  satisfies

$$S(x) - P_{V_0}S(x) = \sum_{j=0}^{\infty} U(2^j x), \text{ where } U(x) = \int \Psi(m)\psi(x-m)dm, \Psi'(x) = 2\psi(x).$$

Proof. The self-similar structure of  $S$  projected on each wavelet scale follows from its homogeneity property  $S(\alpha x) = S(x)$ ,  $\alpha > 0$  and was proven in Lemma 2.3 for all space dimensions. To prove that  $P_{W_0}S(x) = \int \Psi(m)\psi(x-m)dm$  it suffices to compute the respective values of the wavelet transform of  $S$  at the coarsest scale:

$$c_{0,k} = \int S(x)\psi_{0,k}dx = \int_{x<k} \psi_x - \int_{x>k} \psi_x = 2 \int_{x<k} \psi_x = \Psi(k).$$

Inverting the wavelet transform produces the needed expression. ■

Using Theorem 1 and Corollary 2 from Lemma 2.4 we reformulate the above result to obtain the following theorem.

**Theorem 3.1** In the one dimensional case the WGL energy  $\Gamma -$  converges to a constant multiple of TV on the set of characteristic functions  $u = \chi_E$  of finite Borel sets  $E$ :

$$WGL^*(u_\epsilon) \xrightarrow{\Gamma} G_\infty(u) = \frac{\sqrt{3}|\Psi|_{L^2}}{2|\psi * \psi|_{L^2}}|u|_{TV},$$

as  $\epsilon \rightarrow 0$ , w.r.t. the convergence  $u_\epsilon \xrightarrow{L^1} u$ ,  $\{u_\epsilon\} \subset H^1(\mathbb{R})$ .

### 3.2 Explicit form of the WGL $\Gamma$ -limit and the $H^1 - B$ ratio in 2D.

This subsection demonstrates a way to obtain an explicit form of the  $\Gamma$ -limit of WGL on the functions of two variables. Let  $u(x) = \chi_E(x)$  be a characteristic function of a set  $E$  with finite perimeter. First, as an intermediate stage, we consider the case when  $E$  is a polygon. One can see a straightforward connection with the one-dimensional energy if the sides of the polygon are parallel to the coordinate axes. In the general case we determine the connection between the direction of the polygon edges and the respective contributions to the  $B$  and  $H^1$  seminorms of the partial wavelet sums. We establish explicit formulas for the  $\Gamma$ -limit of the WGL (and related  $H^1 - B$  ratio) on characteristic functions of polygons in terms of the direction and size of the edges and the wavelet that was chosen to generate the  $B$ -seminorm.

**Lemma 3.2** Let  $E \subset [0, 1]^2$  be a rectangle with sides parallel to those of the unit square. Then

$$\mathfrak{R}(\chi_E) = \mathfrak{R}(S), \quad \text{where } S \text{ is a unit step function on } \mathbb{R}^1.$$

Proof.

As was shown in the discussion of the general case of polyhedra in  $\mathbb{R}^N$ , the  $\Gamma$ -limit and the respective  $H^1 - B$  ratio are functions of certain values characterizing separate polyhedral faces (Lemmas 2.5, 2.8 ). Those characterizing values are the “densities”  $\rho_B$  and  $\rho_{H^1}$  ( Corollary 1 from Lemma 2.4 ), and  $N - 1$ -dimensional measures of the faces.

The half-planes containing the sides of the rectangle share the same values of  $\rho_B$  and  $\rho_{H^1}$ , because those are invariant with respect to taking the complementary half-plane as well as to switching the variables  $x$  and  $y$ .

Let  $\pi$  be the right half-plane of the coordinate system, then  $\chi_\pi(x, y) = S(x)\mathbb{I}(y)$ . The vertical and diagonal components of its wavelet transform are identically zero, as well as the partial derivative with respect to  $y$ . Computing  $\rho_B$  and  $\rho_{H^1}$  according to Definition 3 we find those are equal to the corresponding values for the one-dimensional step function. ■

### 3.3 $H^1 - B$ ratio as an anisotropic energy functional in two dimensions

In this subsection we find the densities  $\rho_B$  and  $\rho_{H^1}$  in the 2D case specifically, using one-dimensional characteristics of the step function. Moreover, we express those values in formulae of 1D complexity.

#### 3.3.1 Dependence of the Besov seminorm of a partial wavelet sum of an indicator function on the shape of the set boundary

Consider a line  $\lambda$  that forms angle  $\beta$  with the horizontal axis and assume  $0 < \beta < \pi/2$  (the case when  $\beta = 0, \pi/2$  was described in Lemma 3.2). Due to the fact that we use a separable wavelet basis, the dependence of the limiting energy on the edge direction is  $\pi/2$ -periodic.

Since this discussion focuses on the translation invariant (t.i.) Besov seminorm, one can, without loss of generality, assume that the  $\lambda$  passes through the coordinate origin. Let  $\pi$  denote one of the half-planes separated by  $\lambda$ . Then  $\chi_\pi(x, y) = S(y - \tan \beta x)$ .

Using Definition 2 for our case  $N = 2$ , let us denote  $G(x, y) = f_0^\lambda(x, y)$ . The omitted limits of integration below imply that the integration is performed over the maximum applicable domain. We proceed with computing  $\beta_0(f^\lambda)$  via the semi-discrete t.i. dyadic wavelet transform, as an integral of coefficient squares over the corresponding index set:

$$\|f^\lambda\|_{L_{W_0}^2}^2 = \int \int | \int \int S(\cos \beta x + \sin \beta y) \psi^{(1)}(x - k) \psi^{(2)}(y - m) dx dy |^2 dm dk,$$

where  $\psi^{(i)}$  equals  $\psi$  or  $\phi$  depending on the desired wavelet orientation, and the notation itself implies summation over three possible combinations:  $\psi_1 = \psi, \psi_2 = \phi$  (horizontal), or  $\psi_1 = \phi, \psi_2 = \psi$  (vertical), or  $\psi_1 = \psi, \psi_2 = \psi$  (diagonal).

Let us find diagonal, horizontal and vertical components of the energy  $\|f^\lambda\|_{L_{W_0}^2}^2$  using the above model. Let  $t := \tan \beta$ .

$$\begin{aligned} \|f_{diag}^\lambda\|_{L_{W_0}^2}^2 &= \int_0^1 \int_0^1 | \int S(y - xt) \psi(x - k) \psi(y - m) dx dy |^2 dk dm = \int_0^1 | \int S(y - xt) \psi(x) \psi(y - c) dx dy |^2 dc \\ &= \int | \int \Psi(xt - c) \psi(x) dx |^2 dc = \int | \int \Psi(xt) \psi(x + c/t) dx |^2 dc = \\ &= t \int | \int \Psi(xt) \psi(x - c) dx |^2 dc = t \|\Psi(xt)\|_{L_{W_0}^2}^2. \end{aligned}$$

Analogously,

$$\begin{aligned} \|f_{vert}^\lambda\|_{L_{W_0}^2}^2 &= \int | \int S(y - xt) \phi(x) \psi(y - c) dx dy |^2 dc = \int | \int \Psi(xt + c) \phi(x) dy |^2 dc = \\ &= \int | \int \Psi(xt) \phi(y - c/t) dy |^2 dc = t \|\Psi(xt)\|_{L_{V_0}^2}^2. \end{aligned}$$

To compute the horizontal component energy we employ the relation  $S(y - xt) = -S(x - y/t)$  and get

$$\begin{aligned} \|f_{hor}^\lambda\|_{L_{W_0}^2}^2 &= \int | \int S(x - y/t) \psi(x) \phi(y - c) dx dy |^2 dc = \int | \int S(x - y/t) \psi(x) \phi(y - c) dx dy |^2 dc = \\ &= \int | \int \Psi(y/t) \phi(y - c) dy |^2 dc = \int | \int \Psi(y/t) \phi(y - c) dy |^2 dc = \|\Psi(y/t)\|_{L_{V_0}^2}^2. \end{aligned}$$

The line segment that lies within the unit square has length  $(\cos \beta)^{-1}$ . Therefore, according to the definition,

$$(\rho_B)^2(\beta, \psi) = \sin \beta \|\Psi(xt)\|_{L_{W_0}^2}^2 + \sin \beta \|\Psi(xt)\|_{L_{V_0}^2}^2 + \cos \beta \|\Psi(y/t)\|_{L_{V_0}^2}^2, \quad t = \tan \beta.$$



As was mentioned in the proof of lemma 2.7  $\rho_B$  is continuous w.r.t.  $\beta$ . Lemma 3.2 implies

$$(\rho_B)^2(0, \psi) = (\rho_B)^2(\pi/2, \psi) = \|St\|_{L^2_{W_0}}^2 = \|\Psi\|_{L^2}^2,$$

which has no contradiction with the continuity of  $\rho_B$ . Indeed, if  $\beta \rightarrow 0$  the third term in the sum representing  $\rho_B^2(\beta, \psi)$  approaches  $\|\Psi\|_{L^2}^2$  while the first two terms converge to 0 as  $\beta \rightarrow 0$ . If, in its turn,  $\beta \rightarrow \pi/2$ , the second term converges to  $\|\Psi\|_{L^2}^2$  and the other two terms vanish.

### 3.3.2 Dependence of the $H^1$ seminorm of a partial wavelet sum of an indicator function on the shape of the set boundary

In order to determine  $\rho_{H^1}$  in accordance with definition 3, we will find the  $H^1$  seminorm of the function  $G = P_{W_0} f^\lambda$  and show that  $A_\infty^\lambda = 0$ . Using the same notation  $\psi_{(i)}$  (which also implies summation over horizontal, vertical and diagonal components of the wavelet transform) to keep the generalized form of the discussion, consider  $\partial_x G$  in more detail:

$$\begin{aligned} \partial_x G(x, y) &= \int_0^1 \int_0^1 \left[ \int S(y-tx) \psi_{(1)}(y-k) \psi_{(2)}(x-m) dx dy \right] \psi_{(1)}(y-k) \psi'_{(2)}(x-m) dk dm = \\ &= \int_0^1 \int_0^1 \left[ \int \psi_{(1)}(tx-k) \psi_{(2)}(x-m) dx \right] \psi_{(1)}(y-k) \partial_m (-\psi'_{(2)}(x-m)) dk dm = \\ &= \int_0^1 \left[ \int \psi_{(1)}(tx-k) \psi_{(2)}(x) dx \right] \psi_{(1)}(y-k) \psi_{(2)}(x) dk - \int_0^1 \left[ \int \psi_{(1)}(tx-k) \psi_{(2)}(x-1) dx \right] \psi_{(1)}(y-k) \psi_{(2)}(x-1) dk - \\ &\quad - \int_0^1 \int_0^1 \left[ \int \psi_{(1)}(tx-k) \psi'_{(2)}(x-m) dx \right] \psi_{(1)}(y-k) \psi_{(2)}(x-m) dk dm = \\ &= \int_0^1 \left[ \int \psi_{(1)}(tx-k) \psi_{(2)}(x) dx \right] \psi_{(1)}(y-k) \psi_{(2)}(x) dk - \int_0^1 \left[ \int \psi_{(1)}(tx-k) \psi_{(2)}(x-1) dx \right] \psi_{(1)}(y-k) \psi_{(2)}(x-1) dk + \\ &\quad + \int_0^1 \int_0^1 \left[ t \int \psi_{(1)}(tx-k) \psi_{(2)}(x-m) dx \right] \psi_{(1)}(y-k) \psi_{(2)}(x-m) dk dm \quad (dx f_0). \end{aligned}$$

Since the boundary terms resulting from the integration by parts in (dx f0) correspond to a subset of measure zero in the two-dimensional set of wavelet indices  $(k, m)$ , those bring no contribution to the  $L^2$  norm of  $\partial_x G$ :

$$\|\partial_x G\|_{L^2}^2 = \int_0^1 \int_0^1 \left[ t \int \psi_{(1)}(tx-k) \psi_{(2)}(x-m) dx \right]^2 dk dm.$$

Now, analogously to the computation of  $|G|_B^2$ , we will use the fact that the wavelet transform values are repeated along the lines parallel to the edge. We also recall that the length of the edge inside the unit square equals  $(\cos \beta)^{-1}$ .

$$\begin{aligned} \|\partial_x G\|_{L^2}^2 &= \sin \beta \int_0^1 \left[ t \int \psi(tx) \psi(x-m+k/t) dx \right]^2 dm dk + \sin \beta \int_0^1 \left[ t \int \psi(tx) \phi(x-m+k/t) dx \right]^2 dm dk + \\ &+ \cos \beta \int_0^1 \left[ \int \psi(1/ty) \phi(x-k+tm) dx \right]^2 dk dm = \frac{\sin^3 \beta}{\cos^2 \beta} (\|\psi(tx)\|_{L^2_{W_0}}^2 + \|\psi(tx)\|_{L^2_{V_0}}^2) + \cos \beta \|\psi(x/t)\|_{L^2_{V_0}}^2. \end{aligned}$$

By a symmetric argument,

$$\|\partial_y G\|_{L^2}^2 = \frac{\cos^3 \beta}{\sin^2 \beta} (\|\psi(x/t)\|_{L^2_{W_0}}^2 + \|\psi(x/t)\|_{L^2_{V_0}}^2) + \sin \beta \|\psi(tx)\|_{L^2_{V_0}}^2.$$

Therefore,

$$\begin{aligned} (\rho_{H^1})^2(\beta, \psi) &= \frac{\sin^3 \beta}{\cos^2 \beta} (\|\psi(tx)\|_{L^2_{W_0}}^2 + \|\psi(tx)\|_{L^2_{V_0}}^2) + \cos \beta \|\psi(x/t)\|_{L^2_{V_0}}^2 + \\ &\quad + \frac{\cos^3 \beta}{\sin^2 \beta} (\|\psi(x/t)\|_{L^2_{W_0}}^2 + \|\psi(x/t)\|_{L^2_{V_0}}^2) + \sin \beta \|\psi(tx)\|_{L^2_{V_0}}^2 = \\ &= \frac{\sin^3 \beta}{\cos^2 \beta} \|\psi(tx)\|_{L^2_{W_0}}^2 + \frac{\sin \beta}{\cos^2 \beta} \|\psi(tx)\|_{L^2_{V_0}}^2 + \frac{\cos \beta}{\sin^2 \beta} \|\psi(x/t)\|_{L^2_{V_0}}^2 + \frac{\cos^3 \beta}{\sin^2 \beta} \|\psi(x/t)\|_{L^2_{W_0}}^2. \end{aligned}$$

### 3.3.3 Conclusions about the $\Gamma$ -limit of the WGL energy in 2D

The above derivations allow to restate the general theorem in the case of  $\mathbb{R}^2$  using explicit formulae for the components of the  $\Gamma$ -limiting energy. One acquires a straightforward tool to compute the  $\Gamma$ -limit of WGL on any characteristic function  $u = \chi_E$  of a finite perimeter set  $E \subset \mathbb{R}^2$ . Indeed, both expressions for this energy –

$$G_\infty(u) = \frac{\sqrt{3}}{2} \mathfrak{R}(u) |u|_{TV} \text{ where } \mathfrak{R}(u) = \frac{\int_{\partial E} \rho_B^2(\vec{n}(x), \psi) dl(x)}{\int_{\partial E} \rho_{H^1}^2(\vec{n}(x), \psi) dl(x)},$$

and the alternative one,

$$G_\infty(u) = \int_{\partial E} \rho(\vec{n}(x), \psi) dl(x), \text{ where } \rho = \frac{\rho_B}{\rho_{H^1}},$$

- become explicit formulae after one substitutes

$$\rho_{H^1}^2(\beta, \psi) = \frac{\sin^3 \beta}{\cos^2 \beta} \|\psi(tx)\|_{L^2_{w_0}}^2 + \frac{\sin \beta}{\cos^2 \beta} \|\psi(tx)\|_{L^2_{v_0}}^2 + \frac{\cos \beta}{\sin^2 \beta} \|\psi(x/t)\|_{L^2_{w_0}}^2 + \frac{\cos^3 \beta}{\sin^2 \beta} \|\psi(x/t)\|_{L^2_{v_0}}^2, \text{ and}$$

$$\rho_B^2(\beta, \psi) = \sin \beta |\Psi(xt)|_{L^2_{w_0}}^2 + \sin \beta |\Psi(xt)|_{L^2_{v_0}}^2 + \cos \beta |\Psi(y/t)|_{L^2_{w_0}}^2, \text{ where } t = \tan \beta.$$

Numerical application of those formulae and more details on the role of the  $\Gamma$ -limit of the WGL energy in 2D follow in the next section.

## 4 Relation of WGL to the Wulff problem.

### 4.1 The $\Gamma$ -limit of WGL as a surface tension energy in the Wulff problem

In general, the term Wulff problem refers to the problem of minimizing the energy of a fixed-volume object in  $\mathbb{R}^N$  over possible shapes of its  $(N - 1)$ -dimensional surface, while the surface tension energy is not uniformly distributed. A Wulff shape in 2D can be defined as an equilibrium minimal surface for a crystal or drop of fixed volume which has the least anisotropic surface energy.

In the material science, the free energy of the surface of an isolated bounded crystal depends on the orientation of the surface with respect to the crystalline lattice. Thus, the total surface free energy is defined by  $\int f(n(x)) dS(x)$ , where  $n(x)$  is the unit normal to the surface element  $dS(x)$ ,  $f(n)$  is the free energy density in the direction  $n$  and the integral is taken over the entire surface of the crystal. In thermodynamic equilibrium, the crystal takes a shape minimizing the surface free energy. A method for finding the minimizing shape given the energy density  $f(n)$  was first proposed by Wulff and is referred to as Wulff's theorem. He presented a constructive solution to this minimization problem based on the geometry of the surface tension. Given a polar plot of the surface tension density, consider the hyperplanes passing through each point of the surface on this plot orthogonally to the respective radius-vectors. Then the inner convex envelope of those hyperplanes gives the minimizing crystal shape, which, rescaled to the needed volume, leads to the solution of the problem[26].

The study of an anisotropic crystal growing in a melt gives rise to an equation relating the normal velocity of the motion to both the orientation of the crystal and to its curvature. Osher and Merriman [26] proved, that in the case when the outwards normal velocity is equal to  $f(n)$ , for  $f$  the surface tension and  $n$  the unit outwards normal, the asymptotic growth shape is precisely the Wulff crystal, appropriately scaled in time. This shape minimizes the surface energy for a given volume.

Recall that the  $\Gamma$ -limit of the WGL energy in  $\mathbb{R}^N$  can be written in the following form (part (c) of Theorem 1.1):

$$G_\infty(u) = \frac{\sqrt{3}}{2} \int_{\partial E} \rho(\vec{n}(x), \psi) dl(x),$$

where  $\rho = \frac{\rho_B}{\rho_{H^1}} \in [a/b, b/a]$  by construction and  $a$  and  $b$  are the  $H^1 - B$  equivalency constants:  $a|u|_{H^1} \leq |u|_B \leq b|u|_{H^1}$ . Being an integral of some bounded positive density over a closed  $N - 1$ -dimensional surface,  $G_\infty$  can be interpreted as the total free surface energy. It is not rotation invariant, thus making the problem essentially anisotropic, analogous to the minimization of inhomogeneously distributed surface energy. The

anisotropy of WGL and hence its  $\Gamma$ -limit arises from the one of Besov seminorm. The primary source of anisotropy is the way the wavelet kernel in  $\mathbb{R}^2$  is constructed, more precisely, - the fact that wavelet functions have specific orientation in space.

Treating the  $\Gamma$ -limit of WGL as the total energy of the surface, we can approximate the problem of its minimization by the one of minimizing the WGL instead, as  $\epsilon \rightarrow 0$ . Then the respective WGL minimizers form a sequence approximating the  $G_\infty$  minimizer in  $L_1$ .

Let us consider the WGL-based Wulff problem in 2D. Its aim is to minimize the  $\Gamma$ -limiting energy (a weighted TV functional) on the set of characteristic functions  $u = \chi_E$  of the finite perimeter sets  $E \subset \mathbb{R}^2$  with fixed area  $|E| = A$ .

Consider the approximating problem of minimizing the WGL energy on the set of 2D functions  $f : [0, 1]^2 \rightarrow \{0, 1\}$  under the constraint  $m(\{x : f(x) = 1\}) = A$ , where  $0 < A < 1$ . Integrating the constraint into the energy functional subject to minimization, we obtain the problem:

$$u = \operatorname{argmin} \frac{\epsilon}{2} |f|_{B^2} + \frac{1}{4\epsilon} \int f(x, y)^2 (f(x, y) - 1)^2 dx dy + \lambda \left[ \int f(x, y)^2 dx dy - A \right]^2$$

Next step we take is to introduce a modified WGL energy that allows a degree of freedom in handling the anisotropy.

$$WGL^a(f) = \frac{\epsilon}{2} (|f^h|_{B^2} + a_1 |f^v|_{B^2} + a_2 |f^d|_{B^2}) + \frac{1}{4\epsilon} \int f(x, y)^2 (f(x, y) - 1)^2 dx dy \quad (WGL^a)$$

Here  $a_1, a_2 > 0$ . The  $\Gamma$  limit exists in this case due to the same reason as before.

Lemma A.1 in the Appendix implies that minimizers of the modified  $WGL$  ( or  $WGL^a$ ) energy with the area constraint are  $C^\infty$ .

## 4.2 Numerical evidence of $\Gamma$ -convergence: proximity between energies and between minimizers

As was mentioned in Section 4.1, the  $\Gamma$ -limit of WGL , which we denoted  $G_\infty$ , matches the role of the surface tension energy. We will consider the WGL energy as a variational approximation to  $G_\infty$ , compare their values and respective minimizer shapes. In the series of figures (Fig. 4-6) we consider the results of numerical computations done via the 1D formula (according to Section 3.3.3) coupled with those of finding the WGL energy minimizers via the gradient descent method in 2D. Each figure contains four images A-D: (A) the surface tension analogue (the  $\Gamma$ -limit of  $WGL$  or modified  $WGL^a$  based on a weighted B-seminorm) computed via 1D formula; (B) the corresponding Wulff shape found by the classical method we described in Section 4.1 (as a convex inner envelope of the lines tangent to the radius vectors to points of the polar plot of the surface tension); (C) the minimizer of the modified WGL energy with the area constraint found by the gradient descent simulation in 2 (D) matching of the shapes from B and C.

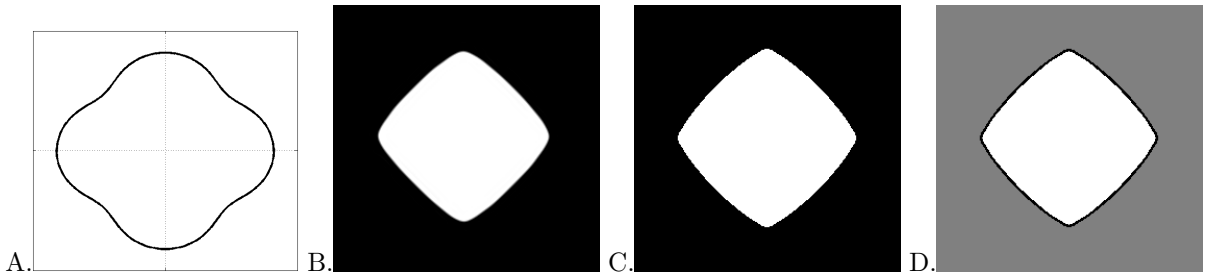


Figure 4: A. Wavelet surface tension analogue  $G_\infty$ ; B. Wulff shape corresponding to A; C. numerically obtained minimizer of the WGL problem with fixed area constraint, image resolution  $256 \times 256$ ,  $\epsilon = 1/100$ ,  $\mu = 1$ ; D. matching B and C - minimizer shapes match up to a rescaling constant.

Two computational examples below consider energies with variable coefficient in front of the diagonal component of the Besov seminorm. As the weight of the diagonal coefficient energy increases, the numerical

convergence slows down making it harder for the approximating  $WGL^a$  minimizer to approach the limiting shape in practical computations, see in particular Fig. 5.

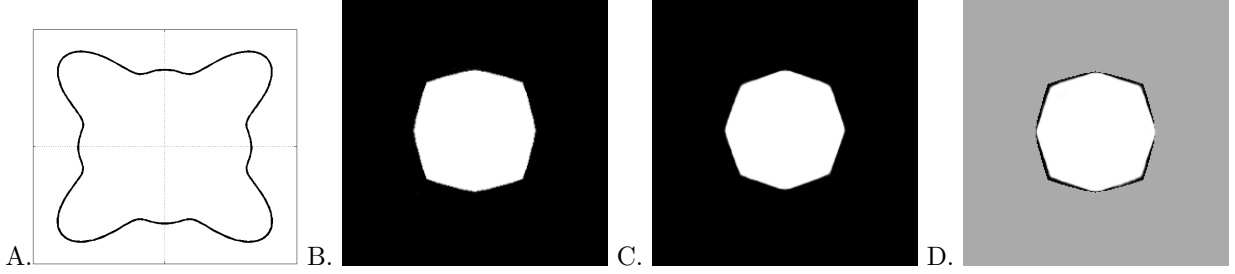


Figure 5: A. Wavelet surface tension analogue -  $\Gamma$  limit of  $WGL^a$ ,  $a_1 = 1, a_2 = 7$ ; B. Wulff shape corresponding to A; C. numerically obtained minimizer of the WGL problem with fixed area constraint, image resolution  $256 \times 256$ ,  $\epsilon = 1/100$ ,  $\mu = 2$ ; D. matching B and C - minimizer shapes match up to a rescaling constant (with minor deviations).

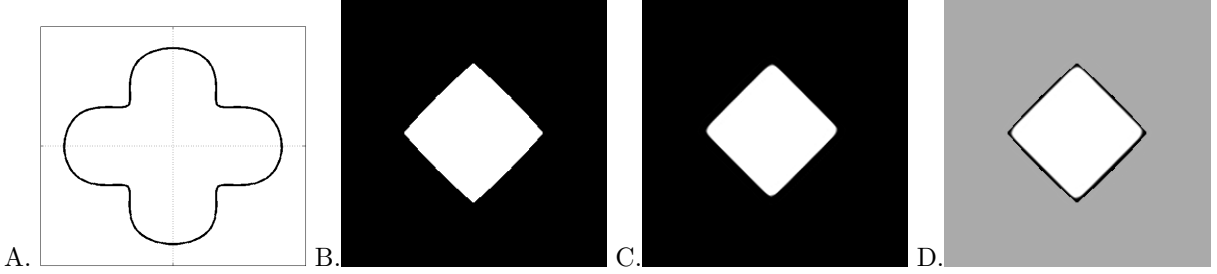


Figure 6: A. Wavelet surface tension analogue -  $\Gamma$  limit of  $WGL^a$ ,  $a_1 = 1, a_2 = 0.1$ ; B. Wulff shape corresponding to A; C. numerically obtained minimizer of the WGL problem with fixed area constraint, image resolution  $256 \times 256$ ,  $\epsilon = 1/32$ ,  $\mu = 1/4$ ; D. matching B and C - minimizer shapes match up to a rescaling constant.

## Acknowledgments

This work was supported by ONR grant N000140810363, NSF grant ACI-0321917, and the Department of Defense.

## A Appendix

### A.1 Rescaling of the classical Ginzburg-Landau energy

Recall that the classical Ginzburg-Landau energy is defined as

$$E_\epsilon(u) = \epsilon \int |\nabla u|^2 dx + \frac{1}{\epsilon} \int W(u) dx, \quad W(u) = (u^2 - 1)^2.$$

We will reformulate the classical result of Lemma 2.1 by introducing the variable rescaling. Let  $u(x) = v(\alpha x)$ , then

$$\int |\nabla u(x)|^2 dx = \int |\nabla v(y)|^2 dy,$$

$$\begin{aligned}\int |\nabla u| dx &= \frac{1}{\alpha} \int |\nabla v(y)| dy, \\ \int W(u) dx &= \frac{1}{\alpha^2} \int W(v(y)) dy.\end{aligned}$$

Rewriting  $E_\epsilon$  as a function of  $v$  produces

$$E_\epsilon^\alpha(v) = \epsilon \int |\nabla v|^2 dx + \frac{1}{\alpha^2 \epsilon} \int W(v) dx.$$

Let us take  $\alpha = \sqrt{2}$  and denote

$$F_\epsilon(u) = \frac{1}{2} E_\epsilon^{\sqrt{2}}(v) = \frac{\epsilon}{2} \int |\nabla u|^2 dx + \frac{1}{4\epsilon} \int W(u) dx.$$

Then, according to the above statement,

$$F_\epsilon \xrightarrow{\Gamma} F(u) = \frac{\sqrt{2}}{3} \int |\nabla u| dx.$$

## A.2 Remark about the $H^1$ and $B$ seminorm equivalency

In the main case we consider  $B$  seminorm is computed via the periodic wavelet transform of function defined on  $[0, 1]^N$ . The periodized scaling function  $\phi$  is identically 1, therefore, the projection of any function on the subspace  $V_0$  brings no contribution to its  $H^1$ -seminorm.

In the case of functions from  $H^1(\mathbb{R}^N)$  the context of our discussion would require defining the  $B$ -seminorm of a function  $u$  as

$$|u|_B = \left( |P_{V_0} u|_{H^1}^2 + \sum_{j=0}^{+\infty} 2^{2j} \int |\langle u, \psi_{j,\mu} \rangle|^2 d\mu \right)^{1/2}.$$

This, however, would not alter the statement of the main theorem or any elements of its proof, since the term  $\epsilon |P_{V_0} u_n|_{H^1}^2$ , where  $u_n \xrightarrow{L^1} u$ , does not contribute anything to the  $\Gamma$ -limit – it converges to 0 as  $\epsilon \rightarrow 0$  for any sequence  $u_n$  approximating  $u = \chi_E$ ,  $E \subset \mathbb{R}^N$ .

## A.3 Semi-continuous dyadic wavelet transform

### A.3.1 Shift-invariant Besov seminorm

We use the semi-continuous wavelet transform with discrete(dyadic) scaling and continuous translation in space rather than the entirely discrete wavelet basis decomposition. The corresponding translation invariant Besov seminorm ( $| \cdot |_{B,t.i.}$ ) can be easily interpreted in terms of the discrete non-redundant wavelet transform that is used to define the usual Besov seminorm ( $| \cdot |_{B,d}$ ). In the argument below we assume all argument shifts to be done over the periodic domain, i.e. all shifts are circular translations modulus 1.

$$\begin{aligned}|u|_{B,t.i.}^2 &= \int_{[0,1]^N} |u(x+h)|_{B,d}^2 dh = \int_{[0,1]^N} \sum_{j=0}^{\infty} 2^{2j} \sum_{k_i=0}^{2^j-1} \left| \int_{[0,1]^N} u(x+h) \psi_{j,k}(x) dx \right|^2 dh = \\ &= \sum_{j=0}^{\infty} 2^{2j} \sum_{k_i=0}^{2^j-1} \int_{[0,1]^N} \left| \int_{[0,1]^N} u(x) \psi_{j,k+2^j h}(x) dx \right|^2 dh = \sum_{j=0}^{\infty} 2^{2j} 2^{Nj} \int_{[0,1]^N} \left| \int_{[0,1]^N} u(x) \psi_{j,2^j h}(x) dx \right|^2 dh \\ &= \sum 2^{2j} \int_{[0,2^j]^N} \left| \int u(x) \psi_{j,\eta}(x) dx \right|^2 d\eta, \quad i = 1, \dots, N.\end{aligned}$$

Our numerical experiments were implemented in Matlab, with the Stationary Wavelet Transform (swt, swt2) routines serving as a substitute for the semi-continuous wavelet transform used in our analysis.

In the actual numerical computations the values of  $h$  are quantized, thus the translation invariant Besov seminorm of a 2D image of size  $2^N \times 2^N$  (rescaled to the domain  $[0, 1]^2$ ) equals

$$|u|_{B, \ell.i., \{2^N \times 2^N\}}^2 = \sum_{j=0}^N 2^{2j} \sum_{k_i=0}^{2^j-1} 2^{-2N} \sum_{m_i=0}^{2^N-1} \left| \int u(x) 2^{-N} \psi_{j, k+2^j m} 2^{-N}(x) dx \right|^2 =$$

$$\sum 2^{4j} 2^{-4N} \sum_{k_i=0}^{2^j-1} \sum_{m_i=0}^{2^{N-j}-1} \left| \int u(x) \psi_{j, k+2^j m} 2^{-N}(x) dx \right|^2 = \sum 2^{-4(N-j)} \sum_{m_i=0}^{2^N-1} \left| \int u(x) \psi_{j, m} 2^{-N}(x) dx \right|^2, \quad i = 1, 2.$$

#### A.4 Regularity of minimizers of the modified WGL energy

We consider minimizers of a modified version of the WGL energy:  $E(u) = WGL(u) + \Lambda(u)$ , whose Euler-Lagrange equation has the following form:

$$\epsilon^2 \Delta_w u - u^3 + u - \lambda(u)u = 0, \quad \lambda(u) \text{ is a constant w.r.t. } x,$$

where  $\Delta_w$  denotes the Wavelet Laplace operator:

$$\Delta_w u(x) = - \sum_{j=0}^{\infty} 2^{2j} \int_0^{2^j} \langle u, \psi_{j,k} \rangle \psi_{j,k}(x) dk$$

One can prove by a standard compactness argument that the energy  $E$  has at least one minimizer. The following lemma shows that all bounded local minimizers are  $C^\infty$  smooth.

**Lemma A.1** *Let a function  $u \in H^1 \cap L^\infty$  be a solution of the above equation (either on  $[0, 1]^N$  with periodic boundary conditions or on  $\mathbb{R}^N$ ), then  $u \in C^\infty$ .*

Proof. Let us project this equation on some wavelet mode  $\psi_{j,k}$ :

$$(\epsilon^2 2^{2j} - 1 + \lambda(u) \langle u, \psi_{j,k} \rangle) = \langle u^3, \psi_{j,k} \rangle.$$

This implies that the values of the wavelet transform  $W(u^3)$  are asymptotically proportional to those of  $W(\Delta_w u)$ . Now,  $u^3 \in H^1$  because

$$|u^3|_{H^1}^2 = \int |\nabla u^3(x)|^2 dx = \int |u^2(x) \nabla u(x)|^2 dx \leq \|u\|_{L^\infty}^4 |u|_{H^1}^2.$$

Hence,  $\Delta_w u \in H^1$ , i.e.  $u \in H^3$ . In general, given  $u \in H^k \cap L^\infty$ , we have  $u^3 \in H^k$ , because

$$|u^3|_{H^k}^2 \leq C \|u\|_{L^\infty}^4 |u|_{H^k}^2.$$

Proceeding to higher order spaces  $H^k$  and performing each step in the same manner as for  $k = 1$  constitutes the "boot-strapping" argument that proves the lemma. ■

## References

- [1] G. Alberti and G. Bellettini. A non-local anisotropic model for phase transitions: asymptotic behaviour of rescaled energies. *Euro. Jnl of Applied Mathematics*, 1(9):261–284, 1998.
- [2] L. Ambrosio and N. Dancer. *Calculus of variations and partial differential equations. Topics on geometrical evolution problems and degree theory*. Springer-Verlag, Berlin-Heidelberg, 2000.
- [3] L. Ambrosio and V. M. Tortorelli. Approximation of functionals depending on jumps by elliptic functionals via  $\Gamma$ -convergence. *Communications on Pure and Applied Mathematics*, XLIII:999–1036, 1990.

- [4] A. Averbuch, G. Beylkin, R. Coifman, and M. Israeli. Multiscale inversion of elliptic operators. In *Signal and image representation in combined spaces*, volume 7 of *Wavelet Anal. Appl.*, page 341359. Academic Press, San Diego, CA, 1998.
- [5] R. W. Balluffi, S. M. Allen, W. C. Carter, and R. A. Kemper. *Kinetics of Material*. John Wiley and Sons, 2005.
- [6] A. Bertozzi, S. Esedoglu, and A. Gillette. Analysis of a two-scale Cahn-Hilliard model for image inpainting. *Multiscale Modeling and Simulation*, 6(3):913–936, 2007.
- [7] A. Bertozzi, S. Esedoglu, and A. Gillette. Inpainting of binary images using the Cahn-Hilliard equation. *IEEE Transactions on Image Processing*, 16(1), January 2007.
- [8] A. Chambolle, R. A. DeVore, N. Lee, and B. J. Lucier. Nonlinear wavelet image processing: Variational problems, compression, and noise removal through wavelet shrinkage. *IEEE Transactions on Image Processing*, 7(3):319–333, 1998.
- [9] T. F. Chan, J. Shen, and H.-M. Zhou. Total variation wavelet inpainting. *Journal of Mathematical Imaging and Vision*, 25(1), July 2006.
- [10] R. R. Coifman and D. L. Donoho. Translation-invariant de-noising. *Lecture Notes in Statistics: Wavelets and Statistics*, New York: Springer-Verlag, 1995.
- [11] W. Dahmen, A. Kurdila, and P. Oswald, editors. *Multiscale Wavelet Methods for Partial Differential Equations*. Wavelet Analysis and Its Applications. Academic Press, 1997.
- [12] I. Daubechies and G. Teschke. Variational image restoration by means of wavelets: simultaneous decomposition, deblurring and denoising. *Applied and Computational Harmonic Analysis*, 19(1):1–16, 2005.
- [13] J. Dobrosotskaya and A. Bertozzi. A wavelet-laplace variational technique for image deconvolution and inpainting. *IEEE Transactions on Image Processing*, 17(5), 2008.
- [14] H. Emmerich. *Diffuse Interface Approach in Materials Science Thermodynamic Concepts and Applications of Phase-Field Models*. Springer books, 2003.
- [15] S. Esedoglu and J. Shen. Digital inpainting based on the Mumford-Shah-Euler image model. *European Journal of Applied Mathematics*, (13):353–370, 2002.
- [16] Selim Esedoglu. "Blind Deconvolution of Bar Code Signals". *Inverse Problems*, (20):121–135, 2004.
- [17] E. De Giorgi. Some remarks on  $\gamma$ -convergence and least squares methods. In G. Dal Maso and G. F DellAntonio, editors, *Composite Media and Homogenization Theory (Proceedings)*, pages 135–142. Birkhauser, 1991.
- [18] E. De Giorgi and T. Franzoni. Su un tipo di convergenza variazionale. *Atti Accad. Naz. Lincei Rend. Cl. Sci. Fis. Mat. Natur.*, (58):842–850, 1975.
- [19] R. Kohn and P. Sternberg. Local minimizers and singular perturbations. pages 69–84. *Proc. Roy. Soc. Edinburgh* 111 A, 1989.
- [20] S. Mallat. *Wavelet Tour of Signal Processing*. Academic Press, September 1999.
- [21] R. March and M. Dozio. A variational method for the recovery of smooth boundaries. *Image and Vision Computing*, 15:705–712, 1997.
- [22] G. Dal Maso. *An introduction to Gamma convergence. Progress in nonlinear differential equations and their applications*. Birkhauser Boston, Inc., Boston, MA, 1993.
- [23] Yves Meyer. *Wavelets and Operators*. Cambridge Univ. Press, 1992.

- [24] L. Modica and S. Mortola. Un esempio di gamma-convergenza. *Boll. Un. Mat. Ital.*, 5(14:1):285–299, 1977.
- [25] I. Ya. Novikov and S. B. Stechkin. Basic wavelet theory. *Russian Mathematical Surveys*, 53:53–128, 1998.
- [26] S. Osher and B. Merriman. The Wulff shape as the asymptotic limit of a growing crystalline interface. *Asian J. Math.*, (3):560–571, September 1997.